# Down-regulation of Polo-like Kinase 1 Elevates Drug Sensitivity of Breast Cancer Cells *In vitro* and *In vivo*

**Birgit Spänkuch, Sandra Heim, Elisabeth Kurunci-Csacsko, Christine Lindenau, Juping Yuan, Manfred Kaufmann, and Klaus Strebhardt**

Department of Obstetrics and Gynecology, Medical School, J.W. Goethe University, Frankfurt, Germany

## Abstract

**Human polo-like kinase 1 (Plk1) is a key player in different stages of mitosis and modulates the spindle checkpoint at the metaphase-anaphase transition. Overexpression of Plk1 is observed in various human tumors and it is a negative prognostic factor in patients suffering from diverse cancers. We used phosphorothioate antisense oligonucleotides (ASO) targeted against Plk1, together with paclitaxel, carboplatin, and Herceptin, for the treatment of breast cancer cells to identify conditions for enhanced drug sensitivity. After transfection of the breast cancer cell lines BT-474, MCF-7, and MDA-MB-435 with Plk1-specific ASOs, paclitaxel, carboplatin, or Herceptin was added and cell proliferation, cell cycle distribution, and apoptosis were measured. Whereas the dual treatment of breast cancer cells with Plk1-specific ASOs with carboplatin or Herceptin caused only a limited antiproliferative effect in breast cancer cells, we observed synergistic effects after combination of low doses of Plk1-specific ASOs with paclitaxel, which is used in a variety of clinical anticancer regimens. Plk1-specific ASOs also acted synergistically with paclitaxel in the arrest of the cell cycle at the $G_2$-M phase and in the induction of apoptosis. Interestingly, in a human xenograft experiment using MDA-MB-435 cells, the combination of Plk1 ASOs with paclitaxel led to synergistic reduction of tumor growth after 3 weeks of treatment compared with either agent alone. This study suggests that antisense inhibitors against Plk1 at well-tolerated doses may be considered as highly efficient promoters for the antineoplastic potential of taxanes, such as paclitaxel, causing synergistic effects in breast cancer cells.** (Cancer Res 2006; 66(11): 5836-46)

## Introduction

Many carcinomas show low susceptibility to antineoplastic drugs, which is a major restriction for chemotherapy of advanced cancers. For this reason, improvements of therapeutic regimens are urgently needed. Recent advances in the field of nucleic acid chemistry offer attractive alternatives to silence gene products important for tumor progression and treatment resistance. Antisense oligonucleotides (ASO) can, when targeted to key elements of proliferation-relevant signal transduction pathways, prevent the development of specific human cancers. Several phosphorothioate ASOs are currently being evaluated in patients suffering from different types of cancer such as ovarian, colon, prostate, lymphoma, non–small-cell lung cancer, chronic myelogenous leukemia, chronic lymphocytic leukemia, and melanomas (1), suggesting ASOs as valuable agents for therapeutic approaches. Furthermore, various investigations used first- and second-generation ASOs targeted against different cancer-relevant genes in combination with traditional chemotherapeutic agents *in vitro* and in clinical trials to enhance the chemosensitivity to various anticancer drugs (2–5).

One cancer-relevant gene is polo-like kinase 1 (*Plk1*), which attracts increasing attention in the field of cancer therapy because this serine/threonine kinase is a key regulator for the mitotic progression of mammalian cells (6) and the activity of Plk1 is elevated in all cancer cells analyzed to date (7, 8). An increasing body of evidence suggests that the level of Plk1 expression has prognostic value for predicting outcomes in patients with several cancers (9). The importance of Plk1 as a measure for the aggressiveness of a tumor seems to result from its important role for the mitotic checkpoints of cancer cells (10–13). Deletion or strong mutations in Plk1-coding genes of different species cause severe growth retardation or even cellular lethality, suggesting that Plks play key roles for the mitotic progression of eukaryotic cells (14, 15). The inhibition of Plk1 led to "mitotic catastrophe" and apoptosis in cancer cells (13, 16–20). In our studies, ASOs or small interfering RNAs reduced Plk1 expression *in vitro* and *in vivo*, leading to defects in centrosomal maturation, increased apoptosis, and tumor inhibition (19–21).

Although antineoplastic agents like carboplatin, paclitaxel, and the monoclonal antibody Herceptin have already exhibited promising results in clinical trials, multiple cases of low susceptibility to these drugs have made treatment decisions by clinicians difficult (22). Thus, the aim of the present study was to combine these agents with ASOs against Plk1 to test conditions for enhanced drug sensitivity in breast cancer cells. Interestingly, the treatment of cancer cells with Plk1-specific ASOs and paclitaxel caused strong inhibition of cell proliferation and tumor growth accompanied by enhanced apoptosis in a synergistic fashion.

## Materials and Methods

**ASOs, antineoplastic agents, and antibodies.** ASOs [Plk1-specific P12 and herpes simplex virus (HSV)–specific as control] were synthesized by MWG Biotech (Ebersberg, Germany; ref. 20). Paclitaxel, carboplatin, and Herceptin were obtained from Roche (Mannheim, Germany).

Monoclonal antihuman Plk1, mouse anti-caspase 3, rabbit anti-caspase 9, goat anti-mouse, and goat anti-rabbit secondary antibodies were purchased from Santa Cruz Biotechnology, Inc. (Heidelberg, Germany), monoclonal antibodies against HER2 from Oncogene Research Products (Calbiochem, Schwalbach, Germany), and monoclonal antibodies against β-actin from Sigma-Aldrich (Taufkirchen, Germany).

**Cell culture.** FCS was purchased from PAA Laboratories (Cölbe, Germany); Leibovitz L15 medium from Sigma-Aldrich; RPMI 1640, PBS,

**Requests for reprints:** Birgit Spänkuch, Department of Obstetrics and Gynecology, Medical School, J.W. Goethe University, Theodor-Stern-Kai 7, D-60590 Frankfurt, Germany. Phone: 49-69-6301-83426; Fax: 49-69-6301-6364; E-mail: Birgit.Spaenkuch@t-online.de.



doi:10.1158/0008-5472.CAN-06-0343

Opti-MEM I, oligofectamine, glutamine, and trypsin from Invitrogen (Karlsruhe, Germany); and bovine insulin from Calbiochem.

The breast cancer cell lines MCF-7 and BT-474 were obtained from DSMZ (Braunschweig, Germany) and MDA-MB-435 from Cell Lines Service (Heidelberg, Germany). All cell lines were cultured according to the instructions of the supplier without antibiotics.

**Treatment and analysis of breast cancer cells.** Cells were transfected with ASOs from 10 to 250 nmol/L using the oligofectamine protocol (Invitrogen) as described (19, 20). Control cells were incubated with Opti-MEM I alone without ASOs or oligofectamine. For combinatorial studies, paclitaxel, carboplatin, or Herceptin was added after the 4-hour transfection period. Concentrations ranged from 0.005 to 10.0 μg/mL culture medium for paclitaxel (23, 24) and Herceptin (25, 26) and from 5 to 200 μg/mL for carboplatin (23).

Cells were harvested 24 hours after the beginning of the transfection period for the analysis of mRNA and 48 hours after the beginning of the transfection period for protein expression, indirect immunofluorescence, and fluorescence activated cell sorting (FACScan). All transfections and combinatorial studies were done in triplicate for each time point. The growth rate of $1.5 \times 10^5$ cells was determined by counting cells at 24, 48, 72, and 96 hours or 2, 6, and 8 days after the beginning of the transfection period or after treatment with drugs as described (19).

**Human cancer xenograft model.** A human cancer xenograft model was established as described (21). In brief, tumor fragments based on MDA-MB-435 breast cancer cells were implanted s.c. into both flanks of nude mice, which were then randomly assigned to six independent treatment groups of six mice. When tumors reached a volume of 80 to 100 $mm^3$, the mice were subjected to systemic treatment with one of the following agents: control (PBS), P12 (1.2 mg/kg bodyweight/d), P12 (12 mg/kg), control HSV (12 mg/kg), paclitaxel (15 mg/kg), and P12 plus paclitaxel (P12 1.2 mg/kg plus paclitaxel 15 mg/kg). The ASOs (P12 and HSV; ref. 20) and paclitaxel were applied at concentrations used in previous analyses (23, 27–29). Injections were carried out i.v. in 100 μL PBS on days 1 to 5, 8 to 12, and 15 to 19. Tumor diameters were measured during the treatment period as described (20) and mean tumor diameters were calculated. One day after the last treatment, animals were sacrificed and tumors were excised for extraction of protein.

Experiments with human cancer xenograft mouse models were approved by the Regierungspräsidium Darmstadt (AZ II 25.3-19C20/15). All experiments were done in certified laboratories of the School of Medicine in Frankfurt.

**RNA preparation and reverse transcription-PCR analysis.** Total RNA from cultured cells was isolated using RNeasy mini-kits according to the protocol of the manufacturer 24 hours after transfection (Qiagen, Hilden, Germany). For reverse transcription-PCR (RT-PCR), the Qiagen OneStep RT-PCR Kit was used according to the instructions of the supplier. Two micrograms of total RNA were added to the PCR mix containing Plk1-specific or glyceraldehyde-3-phosphate dehydrogenase (GAPDH)–specific primers, respectively. Plk1-specific primers with the following sequences were chosen to generate a DNA fragment of ~450 bp in length: aagagatcccggaggtccta and tcattcaggaaaaggttgcc. The RT-reaction was carried out at 50°C for 30 minutes, the initial PCR activation step at 95°C for 15 minutes, and the amplification loop (95°C 30 seconds, 59°C 45 seconds, 72°C 1 minute) was repeated 29 times, followed by a final extension step at 72°C for 10 minutes. GAPDH-specific primers with the following sequences were designed to generate a DNA fragment of ~210 bp: taaagggcatcctgggctacact and ttactccttggaggccatgtagg. The RT-reaction was carried out at 50°C for 30 minutes, the initial PCR activation step at 95°C for 15 minutes, and the amplification loop (95°C 30 seconds, 55°C 30 seconds, 72°C 30 seconds) was repeated 60 times, followed by a final extension step at 72°C for 10 minutes. Resulting DNA fragments were separated on 1% agarose gels and visualized by ethidium bromide staining.

Plk1 expression levels were routinely normalized to levels of GAPDH expression. The resulting GAPDH-normalized Plk1 levels are presented relative to GAPDH-normalized levels in untreated cells.

**Western blot analysis.** For the Western blot analysis, breast cancer cells were lysed 48 hours after transfection or 6 days after treatment with Herceptin and protein concentration was determined as described (19). Xenograft tumors were lysed 1 day after the last treatment as described (21). Total protein (10-50 μg) was separated on 10% Bis-Tris-polyacrylamide gels and then transferred (at 30 V for 1 hour) to Immobilon-P membranes (Millipore, Bedford, MA) according to the Invitrogen protocol. Membranes were incubated for 1 hour in 5% powdered nonfat milk in PBS with monoclonal antibodies against Plk1 (1:100), caspase 3 (1:1,000), caspase 9 (1:100), HER2 (1:250), or β-actin (1:200,000) and for 30 minutes in 5% nonfat dry milk with goat anti-mouse serum or goat anti-rabbit serum (1:2,000) and visualized as described (19). Plk1 protein expression levels were presented as described (19). For Western blot and RT-PCR analysis, Plk1, HER2, GAPDH, and β-actin expression was quantified with a Kodak gel documentation system (1D 3.5; ref. 19).

**DNA staining and fluorescence-activated cell sorting.** Fixation of cells and DNA staining was carried out as described (30). DNA was stained with 2-(4-amidinophenyl)-6-indolecarbamidine dihydrochloride (DAPI; Sigma-Aldrich). Cells were examined with a fluorescence microscope (Leica, Wetzlar, Germany) using a 100× oil immersion objective. Cell cycle distribution was analyzed using a Becton Dickinson FACScan (Heidelberg, Germany; ref. 11).

**Statistical methods.** Each Western blot or RT-PCR experiment was done in triplicate. Means of normalized (i.e., to β-actin or GAPDH) signal intensities and 95% confidence intervals (95% CI) were calculated. Statistical analysis was done with two-way ANOVA (GraphPad Prism, GraphPad Software, Inc., San Diego, California) to consider random effects as described (19).

The combination index was calculated using the following equation: combination index = $(Am)_{50}$ / $(As)_{50}$ + $(Bm)_{50}$ / $(Bs)_{50}$, where $(Am)_{50}$ is the concentration of drug A necessary to achieve a 50% inhibitory effect ($IC_{50}$) in the combination, $(As)_{50}$ is the concentration of the same drug that will produce the identical level of effect alone, $(Bm)_{50}$ is the $IC_{50}$ of drug B in the combination, and $(Bs)_{50}$ is the $IC_{50}$ of drug B after single administration. Combination index >1 indicates antagonism, combination index = 1 indicates an additive effect, and combination index <1 indicates synergy (31, 32).

## Results

### Reduction of Plk1 Expression after Treatment with Plk1-Specific ASOs

At first, we tested the ability and the dose dependence of Plk1-specific ASOs to reduce Plk1 mRNA in different breast cancer cells 24 hours after transfection. P12 at 10 nmol/L did not alter Plk1 mRNA expression in MDA-MB-435 cells but concentrations of 50 to 250 nmol/L P12 significantly reduced Plk1 mRNA levels (Fig. 1*A, top*; 10 nmol/L: reduction to 99%, $P = 0.9$; 50 nmol/L: reduction to 62%, $P < 0.01$; 100 nmol/L: reduction to 46%, $P < 0.05$; 250 nmol/L: reduction to 35%, $P < 0.01$). Alterations of Plk1 mRNA levels by the control ASO HSV were not significant compared with Plk1 mRNA levels in control cells. In BT-474 cells, the inhibition of Plk1 mRNA expression was also achieved by Plk1-specific ASOs (Fig. 1*A, middle*; 10 nmol/L: reduction to 66%, $P < 0.05$, 50 nmol/L: reduction to 65%, $P = 0.056$, 100 nmol/L: reduction to 46%, $P < 0.001$, and 250 nmol/L reduction to 50%, $P < 0.01$). In contrast, in MCF-7 cells only the highest concentration of P12 (250 nmol/L) could reduce Plk1 mRNA in a statistically significant manner (Fig. 1*A, bottom*; 50 nmol/L: 100%; 100 nmol/L: reduction to 85%, $P = 0.1$; 250 nmol/L: reduction to 75%, $P < 0.01$). The control ASO targeted to HSV did not alter Plk1 mRNA levels statistically significantly.

Next we analyzed whether down-regulation of Plk1 mRNA expression was accompanied by a reduction in Plk1 protein expression in MDA-MB-435 cells 48 hours after transfection (Fig. 1*B, top*). P12 at concentrations of 10 to 250 nmol/L significantly reduced Plk1 mRNA levels (10 nmol/L: reduction to

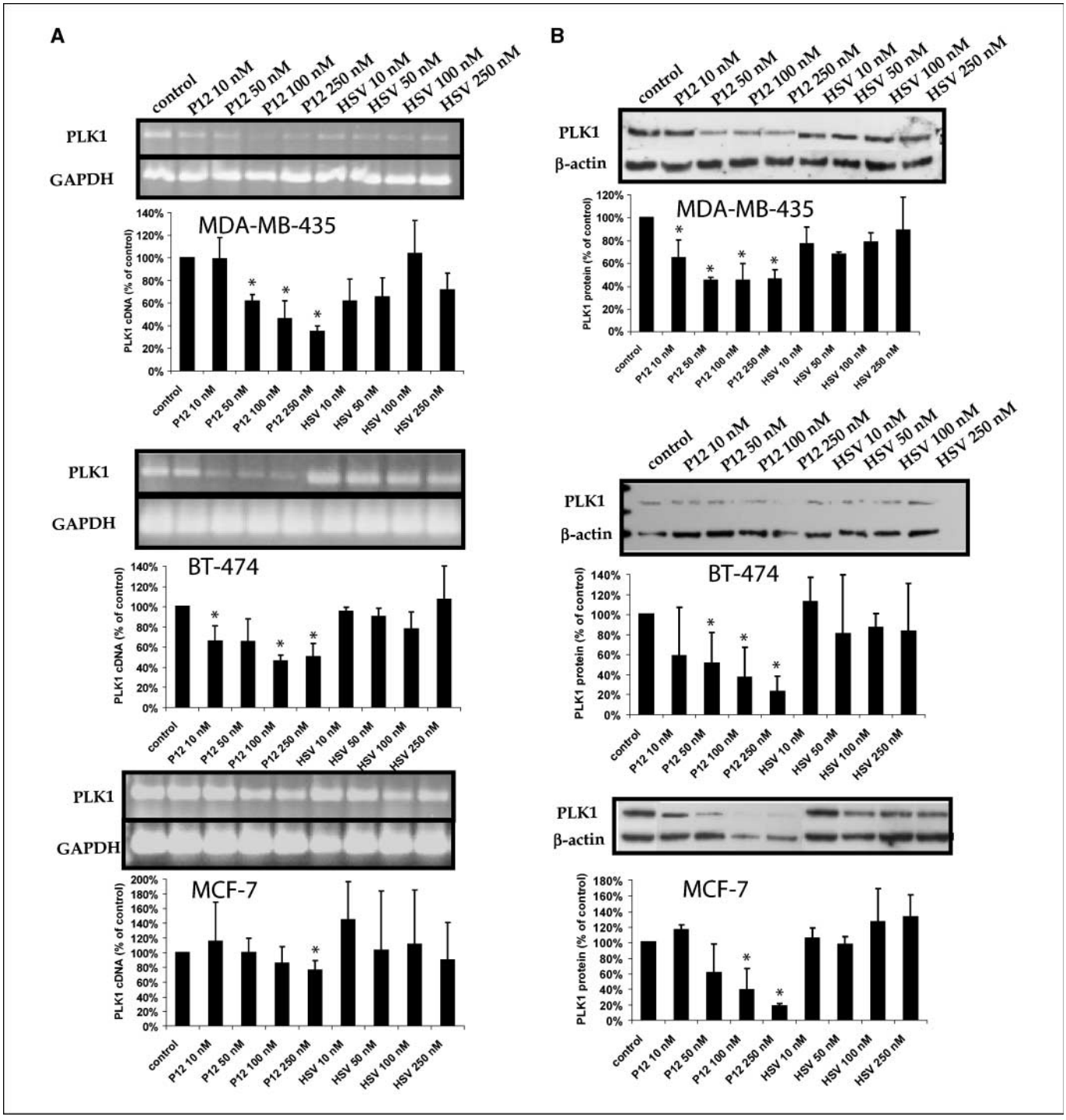


**Figure 1.** RT-PCR and Western blot analysis of MDA-MB-435, MCF-7, and BT-474 cells 24 and 48 hours, respectively, after transfection with Plk1-specific ASOs. Controls were incubated with Opti-MEM I alone. *A,* RT-PCR analysis of MDA-MB-435 (*top*), BT-474 (*middle*), and MCF-7 cells (*bottom*). Each representative gel shows Plk1 cDNA (*top*) and GAPDH cDNA for standardization (*bottom*). Percentage of Plk1 cDNA expression is given as percentage of GAPDH-standardized Plk1 cDNA expression in control cells. *Columns,* mean of three independent experiments; *bars,* 95% CI. *B,* Western blot analysis of MDA-MB-435 (*top*), BT-474 (*middle*), and MCF-7 cells (*bottom*). Each representative Western blot shows Plk1 (*top*) and β-actin protein (*bottom*) for standardization. Percentage of Plk1 protein expression is given as percentage of β-actin-standardized Plk1 levels in control cells. *Columns,* mean of three independent experiments; *bars,* 95% CI.

65%, $P < 0.05$; 50 nmol/L: reduction to 45%, $P < 0.001$; 100 nmol/L: reduction to 45%, $P < 0.01$; 250 nmol/L: reduction to 46%, $P < 0.001$). Down-regulation of the Plk1 protein by the control HSV ASO was weak compared with control cells. In BT-474 cells, 10 nmol/L P12 did not alter Plk1 protein expression significantly but concentrations of 50 to 250 nmol/L P12 significantly reduced Plk1 mRNA levels (Fig. 1*B, middle*; 10 nmol/L: reduction to 58%, $P = 0.1$; 50 nmol/L: reduction to 51%, $P < 0.05$; 100 nmol/L: reduction to 37%, $P < 0.01$; 250 nmol/L: reduction to 23%, $P < 0.001$). In MCF-7 cells, inhibition of Plk1 protein expression was similar compared

with BT-474 cells (Fig. 1*B, bottom*; 10 nmol/L: no reduction of Plk1 protein; 50 nmol/L: reduction to 61%, $P = 0.1$; 100 nmol/L: reduction to 39%, $P < 0.05$; 250 nmol/L reduction to 18%, $P < 0.0001$).

### Reduction of HER2 Protein Expression after Herceptin Treatment

Next we analyzed the expression of the HER2 protein in different breast cancer cell lines by Western blotting. Whereas the level of HER2 was below the limit of detection in MCF-7 and MDA-MB-435 cells, strong expression was observed in BT-474 cells, which is in agreement with previous observations (ref. 33; Fig. 2*A*). Furthermore, we tested whether Herceptin treatment reduces HER2 protein levels in BT-474 cells. Ascending concentrations of Herceptin led to statistically significantly reduced HER2 protein expression 6 days after administration (Fig. 2*B*). Herceptin at 0.01 μg/mL reduced HER2 protein to 91% ($P = 0.1$) but 0.1 μg/mL significantly reduced HER2 protein to 17% ($P < 0.0001$), 1.0 μg/mL to 4% ($P < 0.0001$), and 10.0 μg/mL reduced HER2 protein to 2% ($P < 0.0001$) compared with untreated control cells.

### Antiproliferative Effects of Plk1-Specific ASOs, Paclitaxel, Carboplatin, and Herceptin in Breast Cancer Cells

To study the antiproliferative effect of the Plk1-specific ASO P12 and various antineoplastic agents, the number of breast cancer cells was determined 24, 48, 72, and 96 hours after treatment. Whereas P12 induced only a minor effect at lower concentrations in MDA-MB-435 cells (10 and 50 nmol/L), cell numbers were significantly reduced to 53% at a dose of 100 nmol/L ($P < 0.01$) and to 47% at 250 nmol/L compared with HSV-treated ($P < 0.05$) or untreated control cells ($P < 0.01$; Fig. 3*A, left*). After transfection with P12 at 10 to 250 nmol/L, MCF-7 cells responded with a strong reduction in cell proliferation to levels between 57% and 4% compared with HSV-treated or untreated control cells (Fig. 3*A, middle*; $P < 0.05$ for 50-250 nmol/L). BT-474 cells showed a similar extend of inhibition to levels of 65% to 11% compared with control cells (Fig. 3*A, right*; $P < 0.01$ for all concentrations after 72 hours).

When applying Herceptin at concentrations between 0.01 and 10.0 μg/mL at the same time points as indicated for above-described experiments, proliferation remained unchanged in BT-474 cells (data not shown). Still, 8 days after treatment, cell proliferation decelerated significantly for all analyzed concentrations (Fig. 3*B, right*): 0.01 and 0.1 μg/mL Herceptin reduced cell proliferation to 31% ($P < 0.05$), 1.0 μg/mL to 21% ($P < 0.01$), and 10.0 μg/mL reduced cell proliferation to 10% ($P < 0.001$). In HER2-negative MCF-7 cells, the proliferative activity was independent of the addition of Herceptin (Fig. 3*B, middle*). In HER2-negative MDA-MB-435 cells, only the highest Herceptin concentration of 10.0 μg/mL reduced cell proliferation to levels of 10%, likely due to an unspecific association with the cellular membrane (Fig. 3*B, left*).

Carboplatin induced proliferative inhibition in all breast cancer cell lines analyzed: 10 to 200 μg/mL to 35% to 2% in MDA-MB-435 ($P < 0.001$), to 28% to 4% in MCF-7 ($P < 0.05$), and to 71% to 12% in BT-474 cells ($P = 0.1$-$0.2$) compared with control cells 72 hours after treatment (Fig. 3*C*).

Treatment of breast cancer cell lines with paclitaxel led also to decreased proliferation: In MDA-MB-435 cells, 0.01 μg/mL paclitaxel reduced proliferation to levels of 39%, 0.1 μg/mL to 9%, 1.0 μg/mL to 5%, and 10.0 μg/mL caused complete cell death (Fig. 3*D, left*; $P < 0.01$ for all concentrations after 72 hours). Paclitaxel at concentrations between 0.01 and 10.0 μg/mL reduced proliferation of MCF-7 cells to levels of 30% to 3% compared with controls (Fig. 3*D, middle*; $P < 0.05$ for all concentrations after 72 hours). Paclitaxel reduced proliferation of BT-474 cells to levels between 50% and 7% in a concentration range between 0.01 and 10.0 μg/mL (Fig. 3*D, right*; $P < 0.05$ for 0.01 and 0.1 μg/mL and $P < 0.01$ for 1.0 and 10.0 μg/mL after 72 hours).

### Combinatorial Drug Regimens for the Treatment of Breast Cancer

Combinatorial drug therapy is a treatment paradigm that has proved effective in cancer. But the key, of course, is to identify combinations that yield a benefit at low doses to limit unwanted toxicity. Thus, we tested paclitaxel, carboplatin, and Herceptin, which are already valuable antineoplastic drugs in the clinic, in

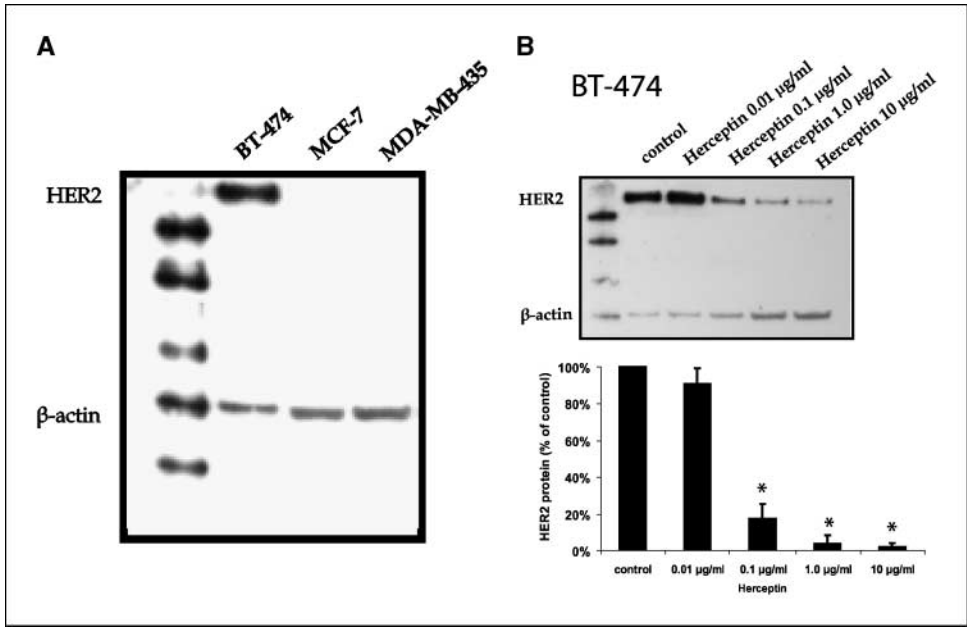


**Figure 2.** *A,* expression of HER2 in breast cancer cell lines. A Western blot analysis was done using anti-HER2 antibodies. To control for variability of loading, membranes were incubated together with antibodies against HER2 and β-actin. *Lanes 1-3,* expression of HER2 in BT-474, MCF-7, and MDA-MB-435 cells. HER2 expression of BT-474 cells after treatment with increasing concentrations of Herceptin. *B,* BT-474 cells were treated with 0.01 to 10.0 μg/mL Herceptin and Western blots were done 6 days after treatment. Membranes were incubated with antibodies against HER2 and β-actin for standardization. Percentage of HER2 protein expression is given as percentage of β-actin-standardized HER2 levels in control cells. *Columns,* mean of three independent experiments; *bars,* 95% CI.

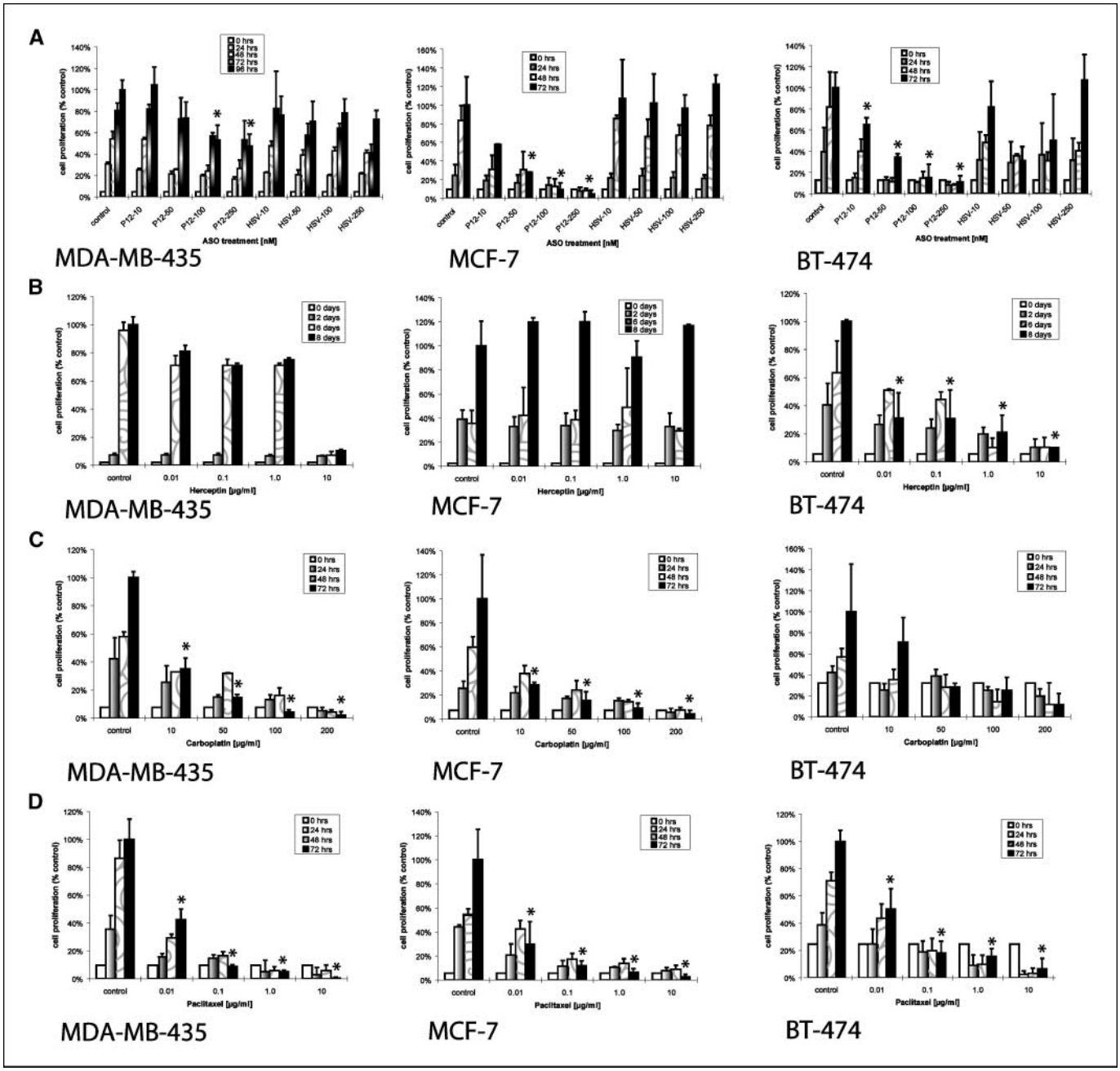


**Figure 3.** Effect of single administration of Plk1 ASOs or antineoplastic drugs on the proliferation of breast cancer cell lines. Controls were incubated with Opti-MEM I alone. *A,* transfection with the ASOs P12 and HSV. MDA-MB-435 (*left*), MCF-7 (*middle*), and BT-474 cells (*right*). *B,* administration of Herceptin alone to MDA-MB-435 (*left*), MCF-7 (*middle*), and BT-474 cells (*right*). *C,* administration of carboplatin alone to MDA-MB-435 (*left*), MCF-7 (*middle*), and BT-474 cells (*right*). *D,* administration of paclitaxel alone to MDA-MB-435 (*left*), MCF-7 (*middle*), and BT-474 cells (*right*). Percentage of surviving cells is given as a percentage of the number of control cells after 72 or 96 hours or after 8 days of incubation, respectively. *Columns,* mean of three different experiments; *bars,* upper 95% CI.

combination with Plk1-specific ASOs to study their effect on cancer cell proliferation and induction of apoptosis. Breast cancer cells were transfected with ASOs 1 day after subcultivation and antineoplastic agents were added after the 4-hour transfection period.

**P12 and Herceptin.** At first, we tested combinatorial effects of Herceptin and the ASO P12. After 2, 6, and 8 days of treatment with 10 nmol/L P12, only a slight decrease in the proliferation of HER2-positive BT-474 cells compared with control cells was measured (Fig. 4*A*). Whereas 8 days was required to gain an inhibitory effect on the proliferation by single administration of Herceptin alone (Fig. 3*C, right*), the combination of 10 nmol/L P12 with 0.005 to 1.0 μg/mL Herceptin led to a proliferative inhibition as early as day 2 and was synergistic (combination index <1).

**P12 and carboplatin.** In MDA-MB-435 cells, 10 nmol/L P12 induced a slight decrease of cell proliferation to 83% compared with control cells ($P = 0.06$; Fig. 4*B, left*). Together with 5 μg/mL carboplatin, proliferation was reduced to 26% after 72 hours ($P < 0.01$), with 10 μg/mL to 9% ($P < 0.01$), with 50 μg/mL to 7% ($P < 0.01$), and with 100 μg/mL to 5% ($P < 0.01$) compared with

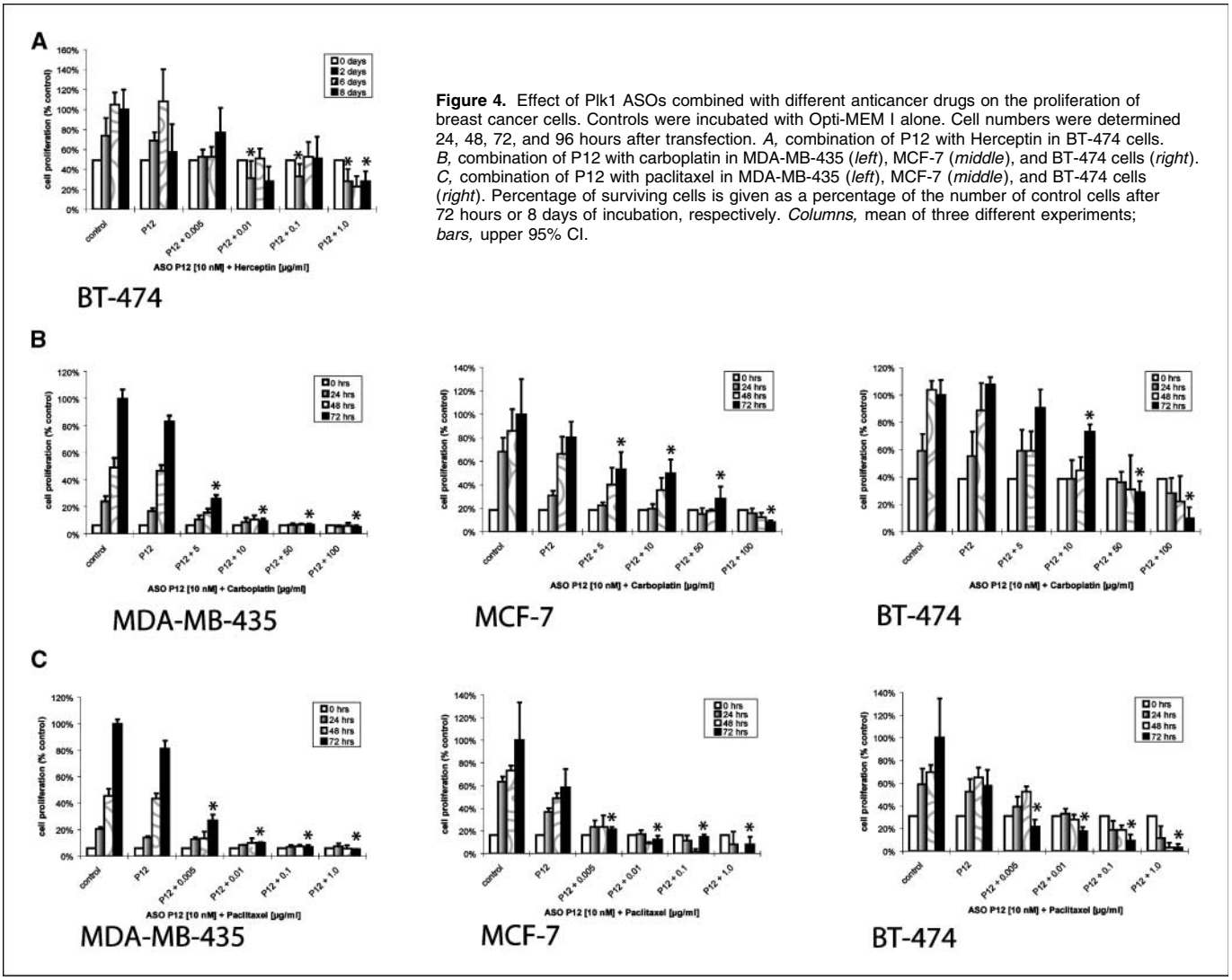


**Figure 4.** Effect of Plk1 ASOs combined with different anticancer drugs on the proliferation of breast cancer cells. Controls were incubated with Opti-MEM I alone. Cell numbers were determined 24, 48, 72, and 96 hours after transfection. *A,* combination of P12 with Herceptin in BT-474 cells. *B,* combination of P12 with carboplatin in MDA-MB-435 (*left*), MCF-7 (*middle*), and BT-474 cells (*right*). *C,* combination of P12 with paclitaxel in MDA-MB-435 (*left*), MCF-7 (*middle*), and BT-474 cells (*right*). Percentage of surviving cells is given as a percentage of the number of control cells after 72 hours or 8 days of incubation, respectively. *Columns,* mean of three different experiments; *bars,* upper 95% CI.

control cells. Whereas the lowest carboplatin concentration tested (5 μg/mL) together with 10 nmol/L P12 slowed down proliferative activity, using 10, 50, and 100 μg/mL carboplatin, respectively, together with 10 nmol/L P12 led to a complete blockade of cell proliferation. Using carboplatin alone, the highest dose of 200 μg/mL induced a complete inhibition of cell proliferation. Thus, these data indicate a synergistic action (combination index <1) of P12 together with carboplatin in MDA-MB-435 cells.

In MCF-7 cells, 10 nmol/L P12 reduced proliferation to 80% after 72 hours ($P = 0.2$) compared with control cells (Fig. 4*B, middle*). In combination with 5 μg/mL carboplatin, proliferation was reduced to 53% after 72 hours ($P < 0.05$), with 10 μg/mL to 50% ($P < 0.05$), with 50 μg/mL to 28% ($P < 0.01$), and with 100 μg/mL to 8% ($P < 0.01$). Carboplatin at 50 and 100 μg/mL together with 10 nmol/L P12 led to a decelerated proliferation, which was also achieved using 100 to 200 μg/mL carboplatin alone. In summary, the combination of Plk1-specific ASOs with carboplatin in MCF-7 cells showed an antagonistic effect (combination index >1).

In BT-474 cells, 10 nmol/L P12 did not reduce proliferation after 72 hours ($P = 0.2$) compared with control cells (Fig. 4*B, right*). P12 at 10 nmol/L in combination with 5 μg/mL carboplatin reduced proliferation to 90% ($P = 0.25$), with 10 μg/mL to 73% ($P < 0.01$), with 50 μg/mL to 29% ($P < 0.001$), and together with 100 μg/mL to 10% ($P < 0.0001$). Whereas the lowest carboplatin concentrations of 5 and 10 μg/mL together with 10 nmol/L P12 did not induce a blockade of proliferation, this effect could be achieved using 50 and 100 μg/mL carboplatin, respectively, in combination with 10 nmol/L P12. This displays an antagonistic effect (combination index >1) compared with single carboplatin administration in BT-474 cells.

**P12 and paclitaxel.** Moreover, we analyzed the effect of low-dose P12 (10 nmol/L) together with paclitaxel in concentrations from 0.005 to 1.0 μg/mL on the proliferation of MDA-MB-435 cells (Fig. 4*C, left*). P12 alone at 10 nmol/L reduced proliferation in MDA-MB-435 cells to 81% ($P < 0.01$) after 72 hours compared with control cells. For comparison, 0.005 μg/mL paclitaxel alone reduced cell proliferation to 70% compared with controls. Interestingly, together with 0.005 μg/mL paclitaxel, 10 nmol/L P12 reduced cell proliferation to 27% ($P < 0.0001$), with 0.01 μg/mL to 10% ($P < 0.0001$), with 0.1 μg/mL to 7% ($P < 0.0001$), and with 1.0 μg/mL to 5% ($P < 0.0001$). In summary, the application of low doses of P12 enhanced the antiproliferative effect exerted by paclitaxel in a synergistic manner (combination index <1).

In MCF-7 cells, 10 nmol/L P12 induced a moderate reduction in proliferation to 59% after 72 hours ($P < 0.05$) compared with control cells (Fig. 4*C, middle*). For comparison, 0.005 μg/mL paclitaxel alone reduced cell proliferation to 60% compared with control cells. In combination with 0.005 μg/mL paclitaxel, proliferation was reduced after 72 hours to 21% ($P < 0.01$), with 0.01 μg/mL to 12% ($P < 0.01$), with 0.1 μg/mL to 15% ($P < 0.01$), and with 1.0 μg/mL to 8% ($P < 0.01$). Even the lowest paclitaxel concentration of 0.005 μg/mL together with 10 nmol/L P12 led to a complete blockade of proliferation, which was only achieved using paclitaxel alone at high concentrations >1.0 μg/mL, indicating a synergistic action (combination index <1).

In BT-474 cells, 10 nmol/L P12 induced a reduction in proliferation to 58% compared with control cells 72 hours after transfection ($P = 0.1$; Fig. 4*C, right*). For comparison, 0.005 μg/mL paclitaxel alone reduced cell proliferation to 79% compared with controls. In combination with 0.005 μg/mL paclitaxel, proliferation was reduced to 22% after 72 hours ($P < 0.05$), with 0.01 μg/mL to 18% ($P < 0.05$), with 0.1 μg/mL to 9% ($P < 0.05$), and with 1.0 μg/mL to 3% ($P < 0.01$). These data substantiate the synergistic action between P12 and paclitaxel (combination index <1).

In summary, our results suggest that the Plk1-specific ASO P12 at low doses together with paclitaxel acts synergistically to inhibit the proliferative activity of three breast cancer cell lines (combination index <1 for all cell lines). For this reason, we analyzed the antiproliferative effect of the Plk1-specific ASO P12 with paclitaxel in subsequent experiments in more detail.

### Induction of Apoptosis in MDA-MB-435 Cells after Treatment with Paclitaxel and Plk1-Specific ASOs

Next we analyzed whether inhibition of proliferation of breast cancer cells induced by Plk1-specific ASOs and/or paclitaxel correlates with apoptosis. We treated MDA-MB-435 cells with ascending doses of paclitaxel (0.01-10.0 μg/mL) and analyzed the induction of apoptosis by monitoring the activation of caspase 3 and caspase 9 in Western blot experiments. Forty-eight hours after paclitaxel treatment, caspase 3, the executioner caspase in apoptosis, and caspase 9 were clearly activated, as shown by the cleavage of full-length protein (Fig. 5*A*). Activation of caspase 9 was statistically significant with 0.01 μg/mL paclitaxel ($P < 0.001$) and with 0.1 μg/mL ($P < 0.001$), 1.0 μg/mL ($P < 0.01$), and 10.0 μg/mL ($P < 0.001$) paclitaxel. Activation of caspase 3 was observed with statistically significant values for 1.0 and 10.0 μg/mL ($P < 0.05$ for both concentrations). Moreover, MDA-MB-435 cells that were transfected with P12, treated with paclitaxel or with a combination of both agents, were stained with DAPI (Fig. 5*B*). Cells treated with 10 nmol/L P12 did not show apoptotic nuclei (data not shown). After transfection with 100 nmol/L P12, we observed apoptotic nuclei and multinucleated cells (Fig. 5*B, second*). Paclitaxel alone (0.1 μg/mL) induced some apoptotic nuclei (Fig. 5*B, third*), but after combinatorial treatment with low doses of P12 (10 nmol/L) together with low doses of paclitaxel (0.005 μg/mL), which alone did not induce apoptosis, we observed an elevated number of apoptotic nuclei and multinucleated cells (Fig. 5*B, bottom*).

### Cell Cycle Distribution of Breast Cancer Cells after Treatment with Plk1-Specific ASOs and Paclitaxel

MDA-MB-435 cells were treated with the ASOs P12 and HSV, paclitaxel, or a combination of P12 with paclitaxel. Cell cycle distribution was analyzed by FACScan analysis. Increasing P12 concentrations caused an elevated percentage of cells in $G_2$-M phase compared with control cells. P12 at 10 nmol/L increased the percentage of cells in $G_2$-M phase from 12.13% in control cells to 18.65% ($P = 0.1$), 50 nmol/L to 18.59% ($P < 0.05$), 100 nmol/L to 17.62% ($P = 0.2$), and 250 nmol/L to 21.93% ($P < 0.05$; Fig. 5*C, left*). The same concentrations of the control ASO against HSV did not alter the cell cycle distribution significantly (data not shown). An increase of cells in $G_2$-M phase induced by increasing concentrations of P12 correlated with an elevated number of apoptotic nuclei (see Fig. 5*B*). This observation is in agreement with a previous report of Nishii et al. (34) describing the link between cells in $G_2$-M phase and increased apoptosis. Treatment with 0.01 to 1.0 μg/mL paclitaxel led to an increased $G_2$-M content of 17.59% to 43.31% ($P < 0.05$ for 0.01 μg/mL, $P < 0.01$ for 0.1 μg/mL; Fig. 5*C, middle*). Combinatorial treatment with 10 nmol/L P12 and paclitaxel (0.005-1.0 μg/mL) led to a much stronger $G_2$-M arrest compared with either agent alone (from 30.80% to 61.42%; $P < 0.05$ for 10 nmol/L P12 + 0.005 μg/mL paclitaxel, $P < 0.001$ for 10 nmol/L P12 + 0.01-1.0 μg/mL paclitaxel; Fig. 5*C, right*), revealing a synergistic effect between P12 and paclitaxel (combination index <1).

### Antitumor Activity of Plk1-Specific ASOs and Paclitaxel

Moreover, we did a MDA-MB-435 xenograft experiment to elucidate whether the synergistic mode of action of the Plk1-specific ASO P12 and paclitaxel observed in cell culture can also be found *in vivo*. We tested the influence of different concentrations of P12, paclitaxel, or both agents together on the growth rate of MDA-MB-435 tumors. Mice were treated on days 1 to 5, 8 to 12, and 15 to 19, and the tumor volume was measured weekly (Fig. 6*A*). Treatment with the control ASO against HSV did not inhibit tumor growth compared with control mice treated with PBS alone (reduction to 71%, $P = 0.55$). Paclitaxel at a dose of 15 mg/kg reduced tumor growth moderately to 58% ($P = 0.32$) compared with untreated mice and mice receiving HSV as control ASO. P12 at a low dose of 1.2 mg/kg had an inhibitory effect on tumor growth to levels of 40% ($P = 0.14$). The high dose of P12 of 12 mg/kg was able to reduce the growth of MDA-MB-435 tumors significantly to 25% compared with control mice ($P < 0.05$).

Most interestingly, in trials using single agents at low doses (1.2 mg/kg P12 or paclitaxel at a concentration of 15 mg/kg), no statistically significant reduction in tumor growth could be reached, but when we applied both agents at the same concentrations as in single-treatment experiments, a statistically significant reduction in tumor growth to levels of 15% ($P < 0.05$) compared with control mice was observed, indicating a synergistic effect (combination index <1) for these agents. Interestingly enough, there was no evidence of toxicity as judged by body weights of mice treated with P12 and paclitaxel alone or in combination.

### Reduced Plk1 Protein Expression and Apoptosis in Tumors after Treatment with Plk1-Specific ASOs and Paclitaxel

One day after the last treatment, tumors were analyzed for Plk1 expression and apoptosis. We observed a statistically significant reduction in Plk1 protein expression compared with control mice (Fig. 6*B*). The lower dose of P12 (1.2 mg/kg) did not reduce tumor Plk1 protein expression significantly compared with control mice (reduction to 85%; $P = 0.52$) but 12 mg/kg reduced Plk1 protein to

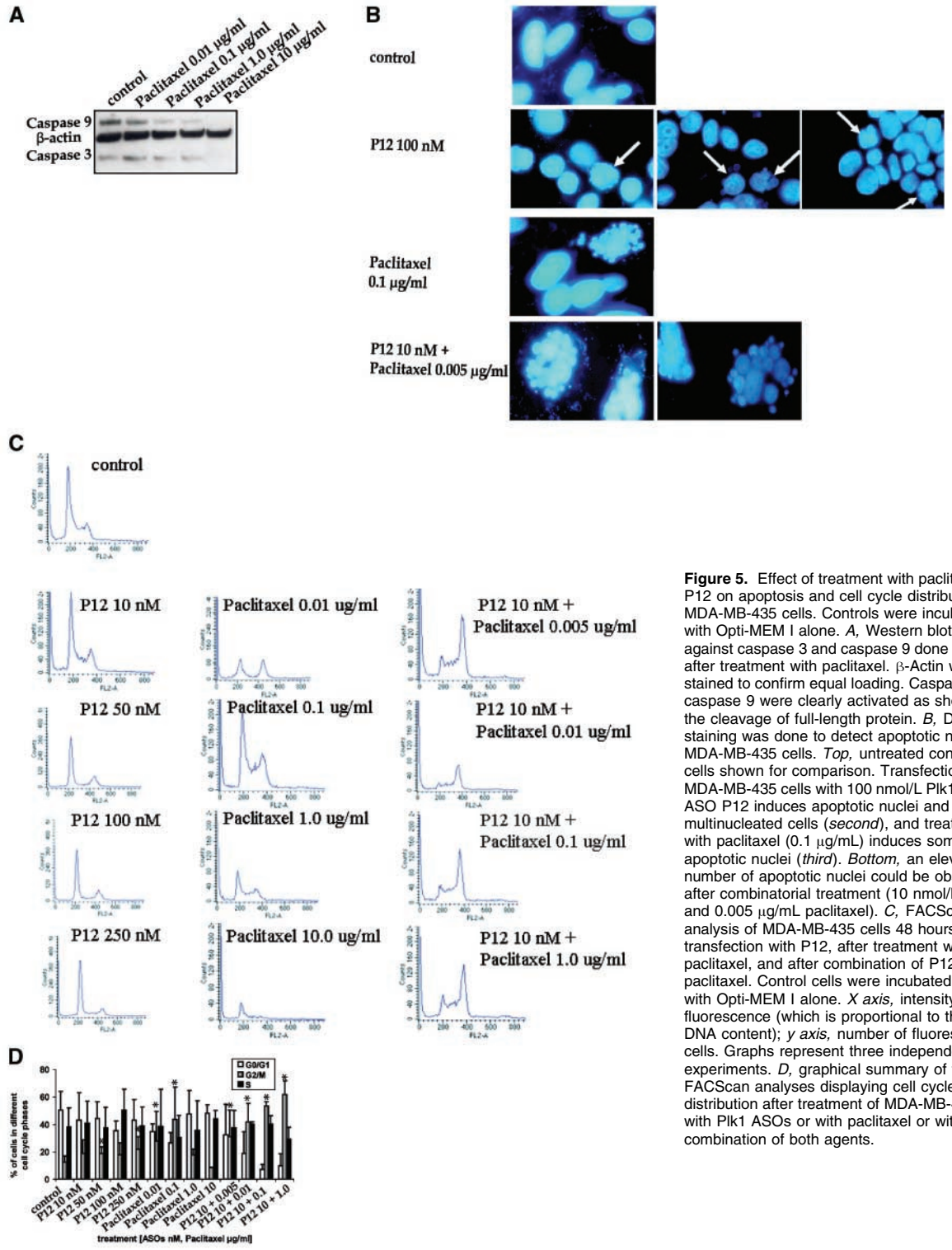


**Figure 5.** Effect of treatment with paclitaxel and P12 on apoptosis and cell cycle distribution of MDA-MB-435 cells. Controls were incubated with Opti-MEM I alone. *A,* Western blot analysis against caspase 3 and caspase 9 done 48 hours after treatment with paclitaxel. β-Actin was stained to confirm equal loading. Caspase 3 and caspase 9 were clearly activated as shown by the cleavage of full-length protein. *B,* DAPI staining was done to detect apoptotic nuclei in MDA-MB-435 cells. *Top,* untreated control cells shown for comparison. Transfection of MDA-MB-435 cells with 100 nmol/L Plk1-specific ASO P12 induces apoptotic nuclei and multinucleated cells (*second*), and treatment with paclitaxel (0.1 μg/mL) induces some apoptotic nuclei (*third*). *Bottom,* an elevated number of apoptotic nuclei could be observed after combinatorial treatment (10 nmol/L P12 and 0.005 μg/mL paclitaxel). *C,* FACScan analysis of MDA-MB-435 cells 48 hours after transfection with P12, after treatment with paclitaxel, and after combination of P12 with paclitaxel. Control cells were incubated with Opti-MEM I alone. *X axis,* intensity of fluorescence (which is proportional to the DNA content); *y axis,* number of fluorescent cells. Graphs represent three independent experiments. *D,* graphical summary of these FACScan analyses displaying cell cycle distribution after treatment of MDA-MB-435 cells with Plk1 ASOs or with paclitaxel or with a combination of both agents.

44% ($P < 0.01$). Paclitaxel at a concentration of 15 mg/kg alone did not influence Plk1 protein expression significantly (reduction to 66%; $P = 0.14$) but the combination of 1.2 mg/kg P12 with paclitaxel led to a statistically significant reduction of Plk1 protein to 37% ($P < 0.01$). This result supports the synergistic mechanism between the Plk1-specific ASO P12 and paclitaxel in mice (combination index <1). In addition, we did Western blot analyses against caspase 3 and caspase 9, which were clearly activated, indicating apoptosis after Plk1 ASO, paclitaxel, or the combinatorial treatment (Fig. 6*C*).

## Discussion

Drug resistance seems to be the main cause for treatment failures in advanced cancers in which a local therapy by surgery and irradiation is insufficient. Only a few types of cancers (e.g., childhood blastomas) can be cured with chemotherapeutic agents (35). However, the effectiveness of chemotherapy on the most widely distributed types of carcinomas of the adult is very unsatisfactory. Obviously, new approaches are needed to overcome resistance to antineoplastic agents. In recent years, the preclinical development of different ASOs targeting cancer-relevant genes has proceeded very rapidly. Many of these have shown convincing *in vitro* reduction in target gene expression and promising activity against a variety of human malignancies. However, on the one hand, inhibition of a single target gene is often not sufficient to suppress tumor growth, considering the multitude of signaling pathways that regulate the proliferation and the life/death decision in cancer cells (36). On the other hand, many ASOs have shown side effects and toxicities in their relevant doses (1, 37). In contrast, clinical trials showed that ASOs at low doses are well tolerated and do not increase the toxicity of conventional treatments. Results from cell culture experiments and from animal models provided convincing evidence that targeted inhibition of genes involved in controlling cell proliferation and apoptosis by ASOs combined with various anticancer drugs is a promising approach for cancer therapy. One of these genes is *Plk1*, which has multiple functions during the cell cycle. After depletion of Plk1 in cancer cells, our studies revealed an elevated number of apoptotic nuclei, an increased sub-2N DNA content, and an increase in $G_2$-M up to 5-fold compared with controls followed by apoptosis (19, 20). Numerous investigations have now established that Plk1 is a prime target candidate for drug development in proliferative diseases such as cancer (9). Thus, we tested the effect of Plk1-specific ASOs alone or in combination with

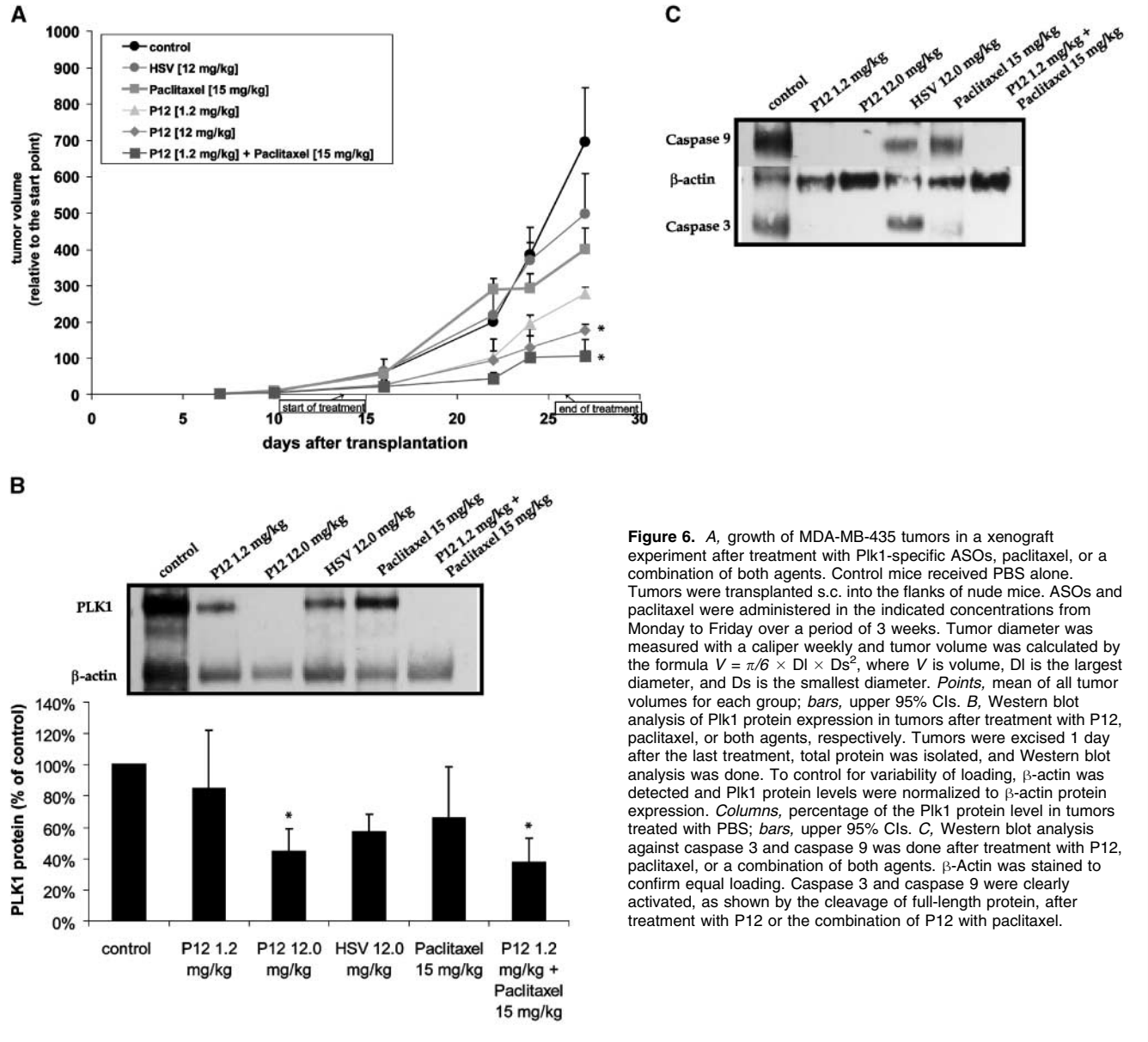


**Figure 6.** *A,* growth of MDA-MB-435 tumors in a xenograft experiment after treatment with Plk1-specific ASOs, paclitaxel, or a combination of both agents. Control mice received PBS alone. Tumors were transplanted s.c. into the flanks of nude mice. ASOs and paclitaxel were administered in the indicated concentrations from Monday to Friday over a period of 3 weeks. Tumor diameter was measured with a caliper weekly and tumor volume was calculated by the formula $V = \pi/6 \times DI \times Ds^2$, where $V$ is volume, DI is the largest diameter, and Ds is the smallest diameter. *Points,* mean of all tumor volumes for each group; *bars,* upper 95% CIs. *B,* Western blot analysis of Plk1 protein expression in tumors after treatment with P12, paclitaxel, or both agents, respectively. Tumors were excised 1 day after the last treatment, total protein was isolated, and Western blot analysis was done. To control for variability of loading, β-actin was detected and Plk1 protein levels were normalized to β-actin protein expression. *Columns,* percentage of the Plk1 protein level in tumors treated with PBS; *bars,* upper 95% CIs. *C,* Western blot analysis against caspase 3 and caspase 9 was done after treatment with P12, paclitaxel, or a combination of both agents. β-Actin was stained to confirm equal loading. Caspase 3 and caspase 9 were clearly activated, as shown by the cleavage of full-length protein, after treatment with P12 or the combination of P12 with paclitaxel.

different antineoplastic agents on the growth of breast cancer cells to search for effective and safe anticancer regimens.

Herceptin is used in metastatic HER2-overexpressing breast cancers, where it leads to response rates of 15% to 40% as single agent (38). In combination with chemotherapeutic drugs like doxorubicin, paclitaxel, or carboplatin, it prolongs survival as first-line therapy in those patients (39). Herceptin acts in a cytostatic manner by blocking and down-modulation of the HER2 receptor and by antibody-dependent cellular cytotoxicity as major mechanism of antibody action (40, 41). In combinatorial studies together with Plk1-specific ASOs, we observed synergistic effects only for a limited period of time. In addition, we tested the platinum complex carboplatin, which induces DNA adducts. It is metabolized and/or degraded in blood to toxic by-products with a half-life time of about 30 hours. Because of this stability, it is, compared with cisplatin, relatively less toxic to kidneys and the peripheral nervous system (42). Combining Plk1-specific ASOs with carboplatin induced synergistic effects only in MDA-MB-435 cells.

The third anticancer drug tested, paclitaxel, belongs to the family of taxanes [paclitaxel (Taxol), docetaxel (Taxotere)] which target microtubule dynamics and which are used for the treatment of a spectrum of cancers. The taxanes bind to a subunit of the tubulin heterodimer that forms cellular microtubules thereby accelerating the polymerization of tubulin, efficiently stabilizing and inhibiting the depolymerization of the microtubules (43, 44). Cells show tetraploidy, a transient arrest in mitosis, and a multinucleated interphase state, followed by apoptosis (45). The spindle checkpoint is elicited by these microtubule-specific drugs through mechanisms that monitor correct spindle formation and tension. In normal cells, this control system ensures that the correct number of chromosomes is distributed to daughter cells and therefore preserves genomic integrity. The spindle checkpoint blocks progression into anaphase until all chromosomes have completely aligned at the metaphase plate (46). Current models propose that the spindle checkpoint proteins, BubR1, Bub1, Bub3, Mad1, Mad2, and Plk1, are components of a sensorial system that monitors lack of tension or attachment between the kinetochore and microtubules of the mitotic spindle (47). In case of lack of tension, a "stopp signal" is transmitted to the mitotic machinery to inhibit progression to anaphase by blocking the anaphase promoting complex. The biochemical background of the stopp signal is not fully understood yet, but unaligned chromosomes preferentially accumulate BubR1, Bub1, and Mad1 at the kinetochores. Once the chromosomes become accurately aligned, the kinetochore localization of these proteins diminishes. It is likely that the checkpoint proteins play a multifunctional role in mitotic progression (48). Sensitivity to paclitaxel was previously shown to correlate with decreased BubR1 protein expression in human cancer lines, including those from breast and ovarian cancer (49). This observation is consistent with an earlier report of increased drug sensitivity after knockdown of BubR1 (50). Thus, drug-sensitive cells were found to lack one or more components. What can be done to make the spindle checkpoint less robust, which would make cancer cells more sensitive to drugs that disrupt microtubule dynamics? A detailed inspection of kinetochore proteins that are important in spindle checkpoint signaling after inhibition of Plk1 by siRNA exhibited a significant reduction in the levels of Mad2, Cenp-E, Hec/Ndc80, and Spc24, whereas Bub1, BubR1, and Crest antigens were not significantly affected (51). Thus, we can hypothesize that down-regulation of Plk1 protein levels and its kinase activity at the kinetochores may stabilize microtubule attachment to kinetochores and contribute to an imbalance of the spindle checkpoint, causing increased sensitivity to microtubule drugs such as paclitaxel. Furthermore, inhibition of Plk1 expression significantly reduced the accumulation of the APC/C activator Cdc20 at kinetochores. These observations provide the mechanistic model for the concerted action of paclitaxel and Plk1-specific ASOs seen in our study. Both drugs induced in all breast cancer cell lines a synergistic antiproliferative effect. In addition, for MDA-MB-435 cells, we observed synergistic effects for the induction of a cell cycle arrest, apoptosis, and reduced tumor growth in a xenograft experiment. Moreover, for a synergistic promotion of the anticancer effect of paclitaxel, low doses of Plk1-specific ASOs (10 nmol/L *in vitro* and 1.2 mg/kg in our xenograft model) are sufficient. In contrast, previous studies targeting other cancer-related genes, such as *bcl-2, c-myc, clusterin, PKCη*, and *mdm2*, required high doses of ASOs *in vitro* between 50 nmol/L and 2 μmol/L (35, 52–55). *In vivo* concentrations in combinatorial experiments ranged from 5 to 25 mg/kg bodyweight (53–57). Thus, paclitaxel combined with low doses of Plk1-specific ASO improves the toxicity profile risk associated with a potent antitumor activity. Taken together, the synergism of Plk1-specific ASOs and paclitaxel may improve clinical concepts for the treatment of breast cancer patients.

## Acknowledgments

Received 1/26/2006; revised 3/28/2006; accepted 4/4/2006.

**Grant support:** Nationales Genomforschungsnetz grant 01GR0431, Deutsche Krebshilfe grant 10-6129, Sander Stiftung, Messer Stiftung, and Deutsche Forschungsgemeinschaft grant SP 1092/1-1.

The costs of publication of this article were defrayed in part by the payment of page charges. This article must therefore be hereby marked *advertisement* in accordance with 18 U.S.C. Section 1734 solely to indicate this fact.

We thank K. Frank for her excellent technical support and R. Knecht and H. Baumann for microscopic support.

## References

1. Gleave ME, Monia BP. Antisense therapy for cancer. Nat Rev Cancer 2005;5:468–79.
2. Morris MJ, Cordon-Cardo C, Kelly WK, et al. Safety and biologic activity of intravenous BCL-2 antisense oligonucleotide (G3139) and taxane chemotherapy in patients with advanced cancer. Appl Immunohistochem Mol Morphol 2005;13:6–13.
3. Marshall J, Chen H, Yang D, et al. A phase I trial of a Bcl-2 antisense (G3139) and weekly docetaxel in patients with advanced breast cancer and other solid tumors. Ann Oncol 2004;15:1274–83.
4. Vansteenkiste J, Canon JL, Riska H, et al. Randomized phase II evaluation of aprinocarsen in combination with gemcitabine and cisplatin for patients with advanced/metastatic non-small cell lung cancer. Invest New Drugs 2005;23:263–9.
5. Gouaze V, Liu YY, Prickett CS, Yu JY, Giuliano AE, Cabot MC. Glucosylceramide synthase blockade down-regulates P-glycoprotein and resensitizes multidrug-resistant breast cancer cells to anticancer drugs. Cancer Res 2005;65:3861–7.
6. Glover DM, Hagan IM, Tavares AA. Polo-like kinases: a team that plays throughout mitosis. Genes Dev 1998;12:3777–87.
7. Golsteyn RM, Schultz SJ, Bartek J, Ziemiecki A, Ried T, Nigg EA. Cell cycle analysis and chromosomal localization of human Plk1, a putative homologue of the mitotic kinases *Drosophila* polo and *Saccharomyces cerevisiae* Cdc5. J Cell Sci 1994;107:1509–17.
8. Holtrich U, Wolf G, Brauninger A, et al. Induction and down-regulation of PLK, a human serine/threonine kinase expressed in proliferating cells and tumors. Proc Natl Acad Sci U S A 1994;91:1736–40.
9. Eckerdt F, Yuan J, Strebhardt K. Polo-like kinases and oncogenesis. Oncogene 2005;24:267–76.
10. Toyoshima-Morimoto F, Taniguchi E, Shinya N, Iwamatsu A, Nishida E. Polo-like kinase 1 phosphorylates cyclin B1 and targets it to the nucleus during prophase. Nature 2001;410:215–20.
11. Yuan J, Eckerdt F, Bereiter-Hahn J, Kurunci-Csacsko E,

Kaufmann M, Strebhardt K. Cooperative phosphorylation including the activity of polo-like kinase 1 regulates the subcellular localization of cyclin B1. Oncogene 2002; 21:8282–92.
12. Toyoshima-Morimoto F, Taniguchi E, Nishida E. Plk1 promotes nuclear translocation of human Cdc25C during prophase. EMBO Rep 2002;3:341–8.
13. Cogswell JP, Brown CE, Bisi JE, Neill SD. Dominant-negative polo-like kinase 1 induces mitotic catastrophe independent of cdc25C function. Cell Growth Differ 2000;11:615–23.
14. Ohkura H, Hagan IM, Glover DM. The conserved Schizosaccharomyces pombe kinase plo1, required to form a bipolar spindle, the actin ring, and septum, can drive septum formation in $G_1$ and $G_2$ cells. Genes Dev 1995;9:1059–73.
15. Llamazares S, Moreira A, Tavares A, et al. polo encodes a protein kinase homolog required for mitosis in *Drosophila*. Genes Dev 1991;5:2153–65.
16. Liu X, Erikson RL. Polo-like kinase (Plk)1 depletion induces apoptosis in cancer cells. Proc Natl Acad Sci U S A 2003;100:5789–94.
17. Ahmad N. Polo-like kinase (Plk) 1: a novel target for the treatment of prostate cancer. FASEB J 2004;18:5–7.
18. Lane HA, Nigg EA. Antibody microinjection reveals an essential role for human polo-like kinase 1 (Plk1) in the functional maturation of mitotic centrosomes. J Cell Biol 1996;135:1701–13.
19. Spankuch-Schmitt B, Bereiter-Hahn J, Kaufmann M, Strebhardt K. Effect of RNA silencing of polo-like kinase-1 (PLK1) on apoptosis and spindle formation in human cancer cells. J Natl Cancer Inst 2002;94:1863–77.
20. Spankuch-Schmitt B, Wolf G, Solbach C, et al. Down-regulation of human polo-like kinase activity by antisense oligonucleotides induces growth inhibition in cancer cells. Oncogene 2002;21:3162–71.
21. Spankuch B, Matthess Y, Knecht R, Zimmer B, Kaufmann M, Strebhardt K. Cancer inhibition in nude mice after systemic application of U6 promoter-driven short hairpin RNAs against PLK1. J Natl Cancer Inst 2004;96:862–72.
22. Crown J, Pegram M. Platinum-taxane combinations in metastatic breast cancer: an evolving role in the era of molecularly targeted therapy. Breast Cancer Res Treat 2003;79 Suppl 1:S11–8.
23. Teicher BA, Menon K, Alvarez E, Galbreath E, Shih C, Faul MM. Antiangiogenic and antitumor effects of a protein kinase Cβ inhibitor in murine lewis lung carcinoma and human Calu-6 non-small-cell lung carcinoma xenografts. Cancer Chemother Pharmacol 2001;48:473–80.
24. Mondesire WH, Jian W, Zhang H, et al. Targeting mammalian target of rapamycin synergistically enhances chemotherapy-induced cytotoxicity in breast cancer cells. Clin Cancer Res 2004;10:7031–42.
25. Pegram MD, Konecny GE, O'Callaghan C, Beryt M, Pietras R, Slamon DJ. Rational combinations of trastuzumab with chemotherapeutic drugs used in the treatment of breast cancer. J Natl Cancer Inst 2004;96: 739–49.
26. Mayfield S, Vaughn JP, Kute TE. DNA strand breaks and cell cycle perturbation in herceptin treated breast cancer cell lines. Breast Cancer Res Treat 2001;70:123–9.
27. Kim SJ, Uehara H, Yazici S, et al. Simultaneous blockade of platelet-derived growth factor receptor and epidermal growth factor receptor signaling and systemic administration of paclitaxel as therapy for human prostate cancer metastasis in bone of nude mice. Cancer Res 2004;64:4201–8.
28. Teicher BA, Menon K, Alvarez E, Shih C, Faul MM. Antiangiogenic and antitumor effects of a protein kinase Cβ inhibitor in human breast cancer and ovarian cancer xenografts. Invest New Drugs 2002;20:241–51.
29. Ueno NT, Bartholomeusz C, Xia W, et al. Systemic gene therapy in human xenograft tumor models by liposomal delivery of the E1A gene. Cancer Res 2002;62: 6712–6.
30. Kauselmann G, Weiler M, Wulff P, et al. The polo-like protein kinases Fnk and Snk associate with a Ca(2+)- and integrin-binding protein and are regulated dynamically with synaptic plasticity. EMBO J 1999;18:5528–39.
31. Dai D, Holmes AM, Nguyen T, et al. A potential synergistic anticancer effect of paclitaxel and amifostine on endometrial cancer. Cancer Res 2005;65:9517–24.
32. Chou TC, Talalay P. Quantitative analysis of dose-effect relationships: the combined effects of multiple drugs or enzyme inhibitors. Adv Enzyme Regul 1984;22: 27–55.
33. Chen X, Yeung TK, Wang Z. Enhanced drug resistance in cells coexpressing ErbB2 with EGF receptor or ErbB3. Biochem Biophys Res Commun 2000;277:757–63.
34. Nishii K, Kabarowski JH, Gibbons DL, et al. ts BCR-ABL kinase activation confers increased resistance to genotoxic damage via cell cycle block. Oncogene 1996; 13:2225–34.
35. Sonnemann J, Gekeler V, Ahlbrecht K, et al. Down-regulation of protein kinase Cη by antisense oligonucleotides sensitises A549 lung cancer cells to vincristine and paclitaxel. Cancer Lett 2004;209:177–85.
36. Dahl E, Sadr-Nabavi A, Klopocki E, et al. Systematic identification and molecular characterization of genes differentially expressed in breast and ovarian cancer. J Pathol 2005;205:21–8.
37. Jason TL, Koropatnick J, Berg RW. Toxicology of antisense therapeutics. Toxicol Appl Pharmacol 2004; 201:66–83.
38. Vogel CL, Cobleigh MA, Tripathy D, et al. Efficacy and safety of trastuzumab as a single agent in first-line treatment of HER2-overexpressing metastatic breast cancer. J Clin Oncol 2002;20:719–26.
39. Slamon DJ, Leyland-Jones B, Shak S, et al. Use of chemotherapy plus a monoclonal antibody against HER2 for metastatic breast cancer that overexpresses HER2. N Engl J Med 2001;344:783–92.
40. Therasse P. Measuring the clinical response. What does it mean? Eur J Cancer 2002;38:1817–23.
41. Clynes RA, Towers TL, Presta LG, Ravetch JV. Inhibitory Fc receptors modulate *in vivo* cytoxicity against tumor targets. Nat Med 2000;6:443–6.
42. Sliesoraitis S, Chikhale PJ. Carboplatin hypersensitivity. Int J Gynecol Cancer 2005;15:13–8.
43. Schiff PB, Horwitz SB. Taxol stabilizes microtubules in mouse fibroblast cells. Proc Natl Acad Sci U S A 1980; 77:1561–5.
44. Jordan MA, Wilson L. Microtubules as a target for anticancer drugs. Nat Rev Cancer 2004;4:253–65.
45. Blajeski AL, Kottke TJ, Kaufmann SH. A multistep model for paclitaxel-induced apoptosis in human breast cancer cell lines. Exp Cell Res 2001;270:277–88.
46. Kops GJ, Weaver BA, Cleveland DW. On the road to cancer: aneuploidy and the mitotic checkpoint. Nat Rev Cancer 2005;5:773–85.
47. Hardwick KG. Checkpoint signalling: Mad2 conformers and signal propagation. Curr Biol 2005;15: R122–4.
48. Weaver BA, Bonday ZQ, Putkey FR, Kops GJ, Silk AD, Cleveland DW. Centromere-associated protein-E is essential for the mammalian mitotic checkpoint to prevent aneuploidy due to single chromosome loss. J Cell Biol 2003;162:551–63.
49. Lee EA, Keutmann MK, Dowling ML, Harris E, Chan G, Kao GD. Inactivation of the mitotic checkpoint as a determinant of the efficacy of microtubule-targeted drugs in killing human cancer cells. Mol Cancer Ther 2004;3:661–9.
50. Ditchfield C, Johnson VL, Tighe A, et al. Aurora B couples chromosome alignment with anaphase by targeting BubR1, Mad2, and Cenp-E to kinetochores. J Cell Biol 2003;161:267–80.
51. Ahonen LJ, Kallio MJ, Daum JR, et al. Polo-like kinase 1 creates the tension-sensing 3F3/2 phosphoepitope and modulates the association of spindle-checkpoint proteins at kinetochores. Curr Biol 2005;15:1078–89.
52. Zhang Z, Li M, Wang H, Agrawal S, Zhang R. Antisense therapy targeting MDM2 oncogene in prostate cancer: Effects on proliferation, apoptosis, multiple gene expression, and chemotherapy. Proc Natl Acad Sci U S A 2003;100:11636–41.
53. Thallinger C, Wolschek MF, Maierhofer H, et al. Mcl-1 is a novel therapeutic target for human sarcoma: synergistic inhibition of human sarcoma xenotransplants by a combination of mcl-1 antisense oligonucleotides with low-dose cyclophosphamide. Clin Cancer Res 2004;10:4185–91.
54. Kim R, Emi M, Tanabe K, Toge T. Preclinical evaluation of antisense bcl-2 as a chemosensitizer for patients with gastric carcinoma. Cancer 2004;101: 2177–86.
55. Emi M, Kim R, Tanabe K, Uchida Y, Toge T. Targeted therapy against Bcl-2-related proteins in breast cancer cells. Breast Cancer Res 2005;7:R940–52.
56. Wang H, Yu D, Agrawal S, Zhang R. Experimental therapy of human prostate cancer by inhibiting MDM2 expression with novel mixed-backbone antisense oligonucleotides: *in vitro* and *in vivo* activities and mechanisms. Prostate 2003;54:194–205.
57. Mewani RR, Tang W, Rahman A, et al. Enhanced therapeutic effects of doxorubicin and paclitaxel in combination with liposome-entrapped ends-modified raf antisense oligonucleotide against human prostate, lung and breast tumor models. Int J Oncol 2004;24: 1181–8.